Title
Chemical Lift-Off Lithography of Metal and Semiconductor Surfaces

Journal
ACS Materials Letters, 2(1)

ISSN
2639-4979

Authors
Cheung, Kevin M
Stemer, Dominik M
Zhao, Chuanzhen
et al.

Publication Date
2020-01-06

DOI
10.1021/acsmaterialslett.9b00438

Peer reviewed

HHS Public Access

Author manuscript

ACS Mater Lett. Author manuscript; available in PMC 2020 May 13.

Published in final edited form as:

ACS Mater Lett. 2020 January 6; 2(1): 76–83. doi:10.1021/acsmaterialslett.9b00438.

Chemical Lift-Off Lithography of Metal and Semiconductor Surfaces

Kevin M. Cheung[1,2], **Dominik M. Stemer**[2,3], **Chuanzhen Zhao**[1,2], **Thomas D. Young**[1,2], **Jason N. Belling**[1,2], **Anne M. Andrews**[1,2,4,*], **Paul S. Weiss**[1,2,3,5,*]

[1]Department of Chemistry and Biochemistry, University of California, Los Angeles, Los Angeles, California 90095, United States

[2]California NanoSystems Institute, University of California, Los Angeles, Los Angeles, California 90095, United States

[3]Department of Materials Science and Engineering, University of California, Los Angeles, Los Angeles, California 90095, United States

[4]Department of Psychiatry and Biobehavioral Sciences, Semel Institute for Neuroscience & Human Behavior, and Hatos Center for Neuropharmacology, University of California, Los Angeles, Los Angeles, California 90095, United States

[5]Department of Bioengineering, University of California, Los Angeles, Los Angeles, California 90095, United States

Abstract

Chemical lift-off lithography (CLL) is a subtractive soft-lithographic technique that uses polydimethylsiloxane (PDMS) stamps to pattern self-assembled monolayers of functional molecules for applications ranging from biomolecule patterning to transistor fabrication. A hallmark of CLL is preferential cleavage of Au-Au bonds, as opposed to bonds connecting the molecular layer to the substrate, *i.e.,* Au-S bonds. Herein, we show that CLL can be used more broadly as a technique to pattern a variety of substrates composed of coinage metals (Pt, Pd, Ag, Cu), transition and reactive metals (Ni, Ti, Al), and a semiconductor (Ge) using straightforward alkanethiolate self-assembly chemistry. We demonstrate high-fidelity patterning in terms of precise features over large areas on all surfaces investigated. We use patterned monolayers as chemical resists for wet etching to generate metal microstructures. Substrate atoms, along with alkanethiolates, were removed as a result of lift-off, as previously observed for Au. We demonstrate the formation of PDMS-stamp-supported bimetallic monolayers by performing CLL

[*]**Corresponding Authors** psw@cnsi.ucla.edu, aandrews@mednet.ucla.edu.

Author Contributions

All authors designed the experiments. KMC, DMS, CZ, TDY, and JNB carried out the experiments. All authors performed data analysis and interpreted the results. KMC, AMA, and PSW wrote the manuscript with input from all authors.

Supporting Information

The Supporting Information is available free of charge on the ACS Publications website at DOI: https://doi.org/10.1021/acsmaterialslett.9b00438

Additional methods, SEM images, atomic force microscopy characterization, and XPS sensitivity factors.

Notes

The authors declare no competing financial interests.

on two different metal surfaces using the same PDMS stamp. By expanding the scope of the surfaces compatible with CLL, we advance and generalize CLL as a method to pattern a wide range of substrates, as well as to produce supported metal monolayers, both with broad applications in surface and materials science.

Graphical Abstract

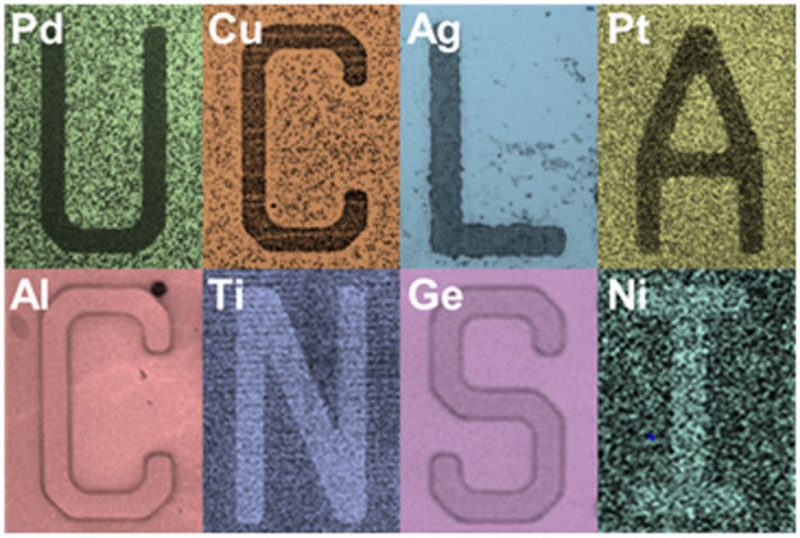

Molecular self-assembled monolayers (SAMs) on surfaces are versatile systems for investigating and tailoring surface, interfacial, and environmental interactions.[1-5] There are a variety of SAM molecules with differing head and tail group functionalities that can be tuned to bind (covalently and noncovalently) and to interact with specific surfaces, with alkanethiol monolayers on Au surfaces representing a commonly used and well-studied system.[6-9] The patterning of alkanethiolate SAMs on metal surfaces imparts an additional level of control and dimension into these systems, which has led to a multitude of applications in surface science and nanotechnology.[1,2,4,6,10-12]

Molecular monolayers can be patterned *via* conventional lithographic techniques (*e.g.*, photolithography),[13,14] but are more commonly patterned using low-cost and high-throughput soft-lithographic methods.[2,3,15,16] Conventional soft lithography (*e.g.*, microcontact printing, μCP), involves the additive patterning of SAM molecules onto surfaces by transfer of molecular inks *via* contact of patterned polydimethylsiloxane (PDMS) stamps with the corresponding surfaces.[17-22] While μCP has significantly advanced the field of SAM patterning, it is inherently limited in the resolution of features produced due to lateral diffusion of ink molecules during and after the patterning is performed.[19,21-24] Advances in soft lithography have improved feature resolution[12-14,25,26] (*e.g.*, polymer pen lithography[27] and microdisplacement printing).[11]

In contrast to abundant additive patterning methods, chemical lift-off lithography (CLL) is a *subtractive* soft-lithographic strategy.[28,29] Here, alkanethiol molecules, with exposed functional tail groups (*e.g.*, -OH, -COOH, $-NH_2$), in preformed SAMs are removed from Au

surfaces only in areas contacted by patterned PDMS stamps.[28-30] Notably, as a result of the CLL process, Au atoms are transferred to the PDMS stamps.[28,29,31] Chemical lift-off lithography enables high-fidelity patterning of SAMs over a wide range of feature sizes (nanometer to millimeter).[28,29,32-34] This patterning process has inspired and enabled diverse applications including the patterning of bioactive molecules,[30,32,35-39] supported gold monolayers,[31] and the facile fabrication of field-effect transistor arrays.[40,41]

Nonetheless, CLL has been primarily used to pattern alkanethiol monolayers on Au surfaces, with the patterning of other coinage, transition, and reactive metal, semiconductor, and metal oxide surfaces representing potentially unexplored areas of interest.[28,42,43] The formation and patterning of alkanethiolate SAMs on other coinage metal surfaces (*e.g.*, Ag, Cu, Pd) have been previously demonstrated using μCP.[6,8,44-52] Alkanthiolate SAMs on transition and reactive metal surfaces are less studied as the reactivity of these surfaces typically leads to the formation of passivating metal oxide layers that hinders additive SAM patterning.[53-57] For subtractive patterning, such as CLL, the entire substrate surface is first functionalized with a SAM, and thus passivated preventing surface oxide formation prior to patterning.[28] Straightforward and direct self-assembly and patterning of molecules on reactive surfaces may be beneficial for a variety of systems including the investigation of spin-selectivity in molecular assemblies on ferromagnetic surfaces,[36,58] patterning of metal-oxide semiconductors for transistor and biosensor applications,[41,59,60] and growth of two-dimensional materials (*e.g.*, graphene nanoribbons).[61,62]

Herein, we extend CLL as a technique to pattern alkanethiolate SAMs on different coinage metals (Pt, Pd, Ag, Cu), transition and reactive metals (Ni, Ti, Al), and a semiconductor (Ge). Using the patterned monolayers as molecular resists, we demonstrate pattern transfer to underlying metal substrates *via* wet etching. In all cases, we show that corresponding supported (mono)layers of substrate atoms are removed during the CLL process. Moreover, we can form atomic blends of mixed metal monolayers on PDMS stamp surfaces. These findings illustrate that CLL is a versatile technique for economical and high-throughput patterning of a multitude of different material surfaces using straightforward alkanethiol self-assembly.

A schematic of the CLL process is shown in Figure 1. Patterned oxygen-plasma-activated PDMS stamps were brought into contact with SAMs of 11-mercapto-1-undecanol (MUO) on metal[28] or semiconductor surfaces. Stamp contact enabled removal of SAM molecules in the contacted substrate areas. We first investigated coinage metals besides Au used in our previous studies (*i.e.*, Pt, Pd, Ag, Cu). Self-assembled monolayers of alkanethiolates have been shown to form on other coinage metals;[44-46,49,63,64] thus, we predicted that CLL could be used to pattern these additional metal surfaces.

Monolayers on metal surfaces were imaged using scanning electron microscopy (SEM) after patterning by CLL. Scanning electron micrographs of Pt, Pd, Ag, and Cu surfaces contacted by “CNSI/UCLA” patterned PDMS stamps showed evidence of negative features in MUO monolayers corresponding to the features of the stamp (Figure 2A-D,S1). Features did not show evidence of broadening associated with lateral diffusion of MUO after patterning,[23] similar to the case of CLL on Au.[33]

Patterned monolayers on metal surfaces after CLL act as molecular resists to facilitate fabrication of metal nano/microstructures *via* chemical wet etching.[28,31,34,40,41] To demonstrate the functionality and resolution of the patterned SAMs, and to confirm that molecules were removed *via* CLL, we exposed patterned metal surfaces to chemical etchants selective for Pt, Pd, Ag, and Cu, respectively (see Methods).[47,48,51,52,65,66] In all cases, metal regions were selectively etched in regions corresponding to areas of SAM removal by CLL, transferring the pattern of the monolayer to the metal substrate (Figure 2E-H). We expect that not all SAM molecules are removed *via* CLL (*ca.* 70% for Au),[28] however sufficient numbers of molecules were removed from all coinage metal surfaces to facilitate selective etching of underlying metals in the lifted-off areas.

Following the observations of coinage metal patterning, we explored extending CLL to transition and reactive metal surfaces (*i.e.*, Ni, Ti, Al), upon which alkanethiolate monolayers can be formed.[53-55] To prevent formation of surface oxides, substrates were immersed into degassed ethanolic MUO solutions to form SAMs immediately after metal evaporation. Since CLL removes regions of preformed SAMs, transition metal surfaces can be patterned straightforwardly without additional surface treatments (*i.e.*, metal oxide etching).[67] Oxide etching roughens metal surfaces,[68] whereas other methods for patterning transition metals, such as SAM displacement, limit the types of molecules that can be patterned (*i.e.*, molecules that are easily displaceable).[11] Transition metal surfaces characterized using SEM indicated that SAMs on these surfaces were patterned using CLL (Figure 3A-C,S1).

We performed CLL on Ge surfaces, a semiconductor that can be functionalized with alkanethiols *via* covalent Ge-S bonds,[68-71] to extend the lithographic capabilities of CLL beyond metals (Figure 3D,S1). Direct patterning of molecules on semiconductor surfaces would foreseeably enable a myriad of applications for semiconductor device processing. For example, local work functions in patterned regions of semiconducting substrates might be tuned for band bending and alignment purposes.[72,73]

We noticed that the contrast observed *via* SEM for the patterned SAMs appears to differ for the different surfaces in Figures 2 and 3. The levels of contrast in SEM for patterned SAMs is related to a variety of factors, including SAM densities and order, as well as the accelerating voltage and working distance of the electron beam during image acquisition.[23,27,31] Given the rapidity of metal oxide formation, we expect that SAMs formed on reactive metal surfaces are not as highly ordered as on coinage metals; trace metal oxides on the former would affect SAM formation.[46,53-57] Differences in SAM formation (*i.e.*, order and density), and thus differences in CLL yield, could contribute to observed differences in contrast. Additionally, formation of oxides in regions of removed SAM molecules after CLL could alter SEM contrast due to differential charging effects.[74-76] Atomic-force microscopy images of patterned SAMs on Ge surfaces showed the expected topographies of monolayers of MUO (Figure S2),[28,31] suggesting that the contrast observed for Ge *via* SEM is mainly an effect of surface compositional differences arising from the patterned SAMs and potentially differential charging effects on the semiconducting surfaces.

To analyze whether substrate molecules were removed during CLL for the metal and semiconductor surfaces investigated herein, similar to previously studied Au substrates,[28,31] X-ray photoelectron spectroscopy (XPS) was performed on PDMS stamps post-CLL. In all cases, characteristic peaks corresponding to the metal or semiconductor substrate atoms were observed (Figure 4), demonstrating that layers of substrate atoms were removed by CLL from all surface types. In some cases, it appeared that layers greater than monolayer were removed (based on the differences in contrast observed in Figure 3, large signal-to-noise differences observed in the XPS spectra in Figure 4, and the relative elemental sensitivities given in Table S1), similar to transfer printing techniques demonstrated by Rogers and others.[77-80]

We previously hypothesized that removal of Au atoms during CLL was partly due to the formation of covalent linkages between the PDMS stamp and SAM molecules, as well as formation of Au-alkanthiolate complexes that weaken the bond strengths between the outermost Au substrate atoms and the underlying Au substrate atoms.[28,31,81] For all elemental substrates tested in this report, the metal-sulfur bonds are stronger than the metal-metal bonds.[82] The energetics of these systems suggest that contributions from differences in bond enthalpies play roles in the removal of the outermost layer(s) of substrate atoms, in addition to adatom formation observed in some monolayer systems.[83] In sum, CLL can be used as a facile top-down method of fabricating and patterning supported metal[62] and semiconductor monolayer materials (*e.g.*, germanane)[84] on flexible and transparent polymer supports such as PDMS.

An advantage of soft lithography is the ability to perform multiple patterning steps to straightforwardly create complex multicomponent patterns.[12,28,39,85] To demonstrate patterning of multiple metals onto the same PDMS support with CLL, we investigated the formation of bimetallic metal layers on PDMS stamps. Previous reports indicated that the PDMS is still activated after a single CLL step (and up to ~5 successive CLL steps using the same stamp on different surfaces), and that full monolayers of Au atoms were not removed onto the PDMS.[28,31,42,86] Taking advantage of this fractional removal, we performed two successive CLL steps on two different metal surfaces (Au and Ag) using the *same* activated PDMS stamp (Figure 5A). X-ray photoelectron spectroscopy of the PDMS stamp after the sequential CLL process showed peaks corresponding to both Au and Ag, demonstrating the formation of mixed-metal monolayers supported on PDMS (Figure 5B-C). Atomically blended bimetallic monolayers represent a new class of materials with unexplored properties and potential applications (*e.g.*, catalysis),[62,87] which can be fabricated straightforwardly using CLL.

In this study, SAMs of the same type of alkanthiolate molecule (MUO) were straightforwardly formed on different metal and semiconductor surfaces. Chemical lift-off lithography is not limited to the surfaces or SAM molecules studied herein;[29,31] presumably, any surface that can be functionalized with molecular monolayers (*e.g.*, metals,[67,88-90] semiconductors,[91] transition metal dichalcogenides)[92] could be patterned with CLL. Performing CLL with molecules containing additional functionalities within the alkyl backbone (*e.g.*, hydrogen-bonding interactions)[93] or functionalized cage molecules (*e.g.*, carboranethiolates),[94-96] which form relatively defect-free monolayers and can have a range

of bond densities between the monolayer and substrate, may have significant effects on the overall efficiencies of CLL.

Monolayers formed on reactive metal surfaces are likely not well ordered due to trace metal oxide formation, yet they can be patterned with *via* CLL. Changing the head group functionality of the SAM molecules to something that binds favorably to surface oxides (*e.g.*, phosphonic acids)[97] can enable the direct patterning of metal oxide surfaces.[42] However, CLL with these types of SAMs, in which the head group is not bound directly to the metal, would be hypothesized not to remove surface metal atoms in the process, but instead break the weakest bonds in the molecules constituting the SAM.[42]

We previously investigated the nanoscale structure and function of supported Au monolayers on PDMS fabricated with CLL and showed that these Au monolayers are ultrathin and optically transparent, yet they retain the chemical functionality of Au.[31] Accordingly, ultrathin monolayers fabricated from other metal and semiconductor surfaces may have chemical and physical properties that can be differentially exploited compared to bulk materials (*e.g.*, magnetism, Ni,[98] semiconductor, Ge).[84] Furthermore, functional metal monolayers could be used as supports for additional structural growth, enabling patterning of a diverse range of materials (*e.g.*, nanoparticles,[99,100] surface-tethered metal-organic frameworks and multilayers,[101-103] and metal-organic chalcogenolate assemblies)[104] on flexible and transparent substrates. Capabilities to create bimetallic and multi-metallic layers and monolayers with CLL adds an additional level of control to the generation and tailoring of supported metal monolayers with designed properties.

Collectively, we demonstrate CLL as a patterning technique that can be used to pattern SAMs on a variety of metal and semiconductor surfaces. Here, high-fidelity patterns of SAMs were generated on coinage, transition, and reactive metal, and semiconductor surfaces beyond Au. Patterned substrates were used as molecular resists for chemical wet etching to produce three-dimensional features. For all surfaces tested, XPS revealed the removal of corresponding substrate atoms during the CLL process. Moreover, reactive and reusable PDMS stamps enable the formation of bimetallic monolayers supported on PDMS by performing two sequential CLL steps on different substrates. Thus, we extend CLL to pattern a variety of surfaces straightforwardly with applications towards the fabrication and study of new materials and systems.

■ Experimental Methods

Materials

Prime quality 4″ Si{100} wafers (P/B, 0.001-0.005 Ω-cm, thickness 500 μm) were purchased from Silicon Valley Microelectronics, Inc. (Santa Clara, CA, USA). Sylgard 184® silicone elastomer kits (lot #0008823745) were purchased from Ellsworth Adhesives (Germantown, WI, USA). 11-Mercapto-1-undecanol was purchased from Sigma Aldrich.

Chemical Lift-Off Lithography

Metal and semiconductor surfaces were prepared *via* electron-beam evaporation (Kurt J. Lesker Company, Jefferson Hills, PA or CHA Industries, SOLUTION, Fremont, CA) onto Si

substrates. Self-assembled monolayers of MUO were formed on metal surfaces *via* immersion in 5 mM ethanolic solutions for 24 h. For reactive metal surfaces (*e.g.*, Cu, Ni, Ti, Al), substrates were immersed in degassed MUO solutions immediately after metal evaporation to minimize metal oxide formation. For Ge, SAMs were formed *via* immersion into a 1:1 (v/v) ethanol:water solution of MUO. Chemical lift-off lithography was performed as previously reported,[28,31] where surfaces were contacted with patterned or featureless oxygen-plasma-activated PDMS stamps for 24 h, after which the stamps were removed. To form supported bimetallic monolayers, featureless PDMS stamps were brought into contact with functionalized Au surfaces for 1 h and then functionalized Ag surfaces for an additional 1 h immediately after lift-off from Au surfaces.

Scanning Electron Microscopy

Scanning electron microscopy images were obtained using a Zeiss Supra 40VP scanning electron microscope with an Inlens secondary electron detector. Surfaces were imaged immediately after CLL. Accelerating voltages were adjusted for each metal surface to produce optimal contrast: 1 kV for Ni, Ti, and Al; 1.5 kV for Pt; 2 kV for Pd, Ag, and Cu; and 3 kV for Ge. Working distances were optimized for each image. Modulating accelerating voltages and working distances affect the contrast observed for patterned SAMs.[23] Images were processed *via* polynomial background subtraction using Gwyddion[105] and contrast limited adaptive histogram equalization in MATLAB.[106]

Metal Etching

Patterned metal surfaces were etched with corresponding chemical wet etchants: Pt with concentrated *aqua regia* (3:1 v/v 12.1 M HCl:15.6 M HNO_3) for 20 min,[66] Pd with a solution of 0.2 M $K_2Cr_2O_7$ and 0.5 M HCl in 40% aqueous H_3PO_4 for 6 min,[107] Ag with an aqueous 25 mM $FeNO_3$ solution for 15 min,[51] and Cu with an aqueous 12 mM $FeCl_3$ solution for 30 s.[52]

X-Ray Photoelectron Spectroscopy

X-ray photoelectron spectroscopy of PDMS surfaces post-CLL was carried out using an AXIS Ultra DLD photoelectron spectrometer (Kratos Analytical Inc., Chestnut Ridge, NY) and a monochromatic Al K_α X-ray source with a 200 μm circular spot size in ultrahigh vacuum (10^{-9} Torr). High-resolution spectra of Au 4f, Pt 4f, Pd 3d, Ag 3d, Cu 2p, Ni 2p, Ti 2p, Al 2p, and Ge 3d regions were acquired at a pass energy of 20 eV using a 300 ms dwell time. For all scans, 15 kV was applied with an emission of 15 mA. An average of 30 scans were collected for each of the high-resolution spectra. Note, all spectra were collected under charge neutralization conditions (*i.e.*, electron flood gun)[58] to prevent charging of sample surfaces. Charge neutralization results in shifts of binding energy values.

Supplementary Material

Refer to Web version on PubMed Central for supplementary material.

■ ACKNOWLEDGMENTS

This research was supported by funding from the National Institute on Drug Abuse (DA045550). KMC thanks the Department of Chemistry and Biochemistry at UCLA for a SG fellowship. The authors thank Dr. John M. Abendroth for assistance with Ni patterning and characterization, Dr. Natcha Wattanatorn for assistance with metal evaporation, and Profs. Mary Elizabeth Anderson, J. Nathan Hohman, and Xiaobin Xu, and Drs. Andrew Serino, Liane Slaughter, and Qing Yang for helpful discussions. The authors acknowledge the use of instruments at the UCLA Molecular Instrumentation Center and Electron Imaging Center and Nano & Pico Characterization Lab at the California NanoSystems Institute.

■ REFERENCES

(1). Wilbur JL; Kumar A; Kim E; Whitesides GM Microfabrication by Microcontact Printing of Self-Assembled Monolayers. Adv. Mater 1994, 6, 600–604.

(2). Mrksich M; Whitesides GM Patterning Self-Assembled Monolayers Using Microcontact Printing: A New Technology for Biosensors? Trends Biotechnol. 1995, 13, 228–235.

(3). Smith RK; Lewis PA; Weiss PS Patterning Self-Assembled Monolayers. Prog. Surf. Sci. 2004, 75, 1–68.

(4). Gates BD; Xu Q; Stewart M; Ryan D; Willson CG; Whitesides GM New Approaches to Nanofabrication: Molding, Printing, and Other Techniques. Chem. Rev 2005, 105, 1171–1196. [PubMed: 15826012]

(5). Braunschweig AB; Huo F; Mirkin CA Molecular Printing. Nat. Chem 2009, 1, 353–358. [PubMed: 21378889]

(6). Love JC; Estroff LA; Kriebel JK; Nuzzo RG; Whitesides GM Self-Assembled Monolayers of Thiolates on Metals as a Form of Nanotechnology. Chem. Rev 2005, 105, 1103–1170. [PubMed: 15826011]

(7). Claridge SA; Liao W-S; Thomas JC; Zhao Y; Cao HH; Cheunkar S; Serino AC; Andrews AM; Weiss PS From the Bottom Up: Dimensional Control and Characterization in Molecular Monolayers. Chem. Soc. Rev 2013, 42, 2725–2745. [PubMed: 23258565]

(8). Vericat C; Vela ME; Corthey G; Pensa E; Cortés E; Fonticelli MH; Ibañez F; Benitez GE; Carro P; Salvarezza RC Self-Assembled Monolayers of Thiolates on Metals: A Review Article on Sulfur-Metal Chemistry and Surface Structures. RSC Adv. 2014, 4, 27730–27754.

(9). Bent SF Heads or Tails: Which Is More Important in Molecular Self-Assembly? ACS Nano 2007, 1, 10–12. [PubMed: 19203125]

(10). Kumar A; Whitesides GM Features of Gold Having Micrometer to Centimeter Dimensions Can Be Formed through a Combination of Stamping with an Elastomeric Stamp and an Alkanethiol ‘‘Ink’’ Followed by Chemical Etching. Appl. Phys. Lett. 1993, 63, 2002–2004.

(11). Dameron AA; Hampton JR; Smith RK; Mullen TJ; Gillmor SD; Weiss PS Microdisplacement Printing. Nano Lett. 2005, 5, 1834–1837. [PubMed: 16159233]

(12). Mullen TJ; Srinivasan C; Hohman JN; Gillmor SD; Shuster MJ; Horn MW; Andrews AM; Weiss PS Microcontact Insertion Printing. Appl. Phys. Lett 2007, 90, 063114.

(13). Anderson ME; Srinivasan C; Hohman JN; Carter EM; Horn MW; Weiss PS Combining Conventional Lithography with Molecular Self-Assembly for Chemical Patterning. Adv. Mater 2006, 18, 3258–3260.

(14). Srinivasan C; Anderson ME; Carter EM; Hohman JN; Bharadwaja SSN; Trolier-McKinstry S; Weiss PS; Horn MW Extensions of Molecular Ruler Technology for Nanoscale Patterning. J. Vac. Sci. Technol., B 2006, 24, 3200–3204.

(15). Xia Y; Whitesides GM Soft Lithography. Angew. Chem. Int. Ed 1998, 37, 550–575.

(16). Rogers JA; Nuzzo RG Recent Progress in Soft Lithography. Mater. Today 2005, 8, 50–56.

(17). Jackman RJ; Wilbur JL; Whitesides GM Fabrication of Submicrometer Features on Curved Substrates by Microcontact Printing. Science 1995, 269, 664–666. [PubMed: 7624795]

(18). Wilbur JL; Kumar A; Biebuyck HA; Kim E; Whitesides GM Microcontact Printing of Self-Assembled Monolayers: Applications in Microfabrication. Nanotechnology 1996, 7, 452–457.

(19). Xia Y; Whitesides GM Extending Microcontact Printing as a Microlithographic Technique. Langmuir 1997, 13, 2059–2067.

(20). Quist AP; Pavlovic E; Oscarsson S Recent Advances in Microcontact Printing. Anal. Bioanal. Chem 2005, 381, 591–600. [PubMed: 15696278]

(21). Alom Ruiz S; Chen CS Microcontact Printing: A Tool to Pattern. Soft Matter 2007, 3, 168–177.

(22). Perl A; Reinhoudt DN; Huskens J Microcontact Printing: Limitations and Achievements. Adv. Mater 2009, 21, 2257–2268.

(23). Srinivasan C; Mullen TJ; Hohman JN; Anderson ME; Dameron AA; Andrews AM; Dickey EC; Horn MW; Weiss PS Scanning Electron Microscopy of Nanoscale Chemical Patterns. ACS Nano 2007, 1, 191–201. [PubMed: 19206649]

(24). Schwartz JJ; Hohman JN; Morin EI; Weiss PS Molecular Flux Dependence of Chemical Patterning by Microcontact Printing. ACS Appl. Mater. Interfaces 2013, 5, 10310–10316.

(25). Piner RD; Zhu J; Xu F; Hong S; Mirkin CA "Dip-Pen" Nanolithography. Science 1999, 283, 661–663. [PubMed: 9924019]

(26). Huo F; Zheng G; Liao X; Giam LR; Chai J; Chen X; Shim W; Mirkin CA Beam Pen Lithography. Nat. Nanotechnol 2010, 5, 637–640. [PubMed: 20676088]

(27). Huo F; Zheng Z; Zheng G; Giam LR; Zhang H; Mirkin CA Polymer Pen Lithography. Science 2008, 321, 1658–1660. [PubMed: 18703709]

(28). Liao W-S; Cheunkar S; Cao HH; Bednar HR; Weiss PS; Andrews AM Subtractive Patterning *via* Chemical Lift-Off Lithography. Science 2012, 337, 1517–1521. [PubMed: 22997333]

(29). Andrews AM; Liao W-S; Weiss PS Double-Sided Opportunities Using Chemical Lift-Off Lithography. Acc. Chem. Res 2016, 49, 1449–1457. [PubMed: 27064348]

(30). Cao HH; Nakatsuka N; Liao W-S; Serino AC; Cheunkar S; Yang H; Weiss PS; Andrews AM Advancing Biocapture Substrates *via* Chemical Lift-Off Lithography. Chem. Mater 2017, 29, 6829–6839.

(31). Slaughter LS; Cheung KM; Kaappa S; Cao HH; Yang Q; Young TD; Serino AC; Malola S; Olson JM; Link S; Häkkinen H; Andrews AM; Weiss PS Patterning of Supported Gold Monolayers *via* Chemical Lift-Off Lithography. Beilstein J. Nanotechnol 2017, 8, 2648–2661. [PubMed: 29259879]

(32). Chen C-Y; Wang C-M; Li H-H; Chan H-H; Liao W-S Wafer-Scale Bioactive Substrate Patterning by Chemical Lift-Off Lithography. Beilstein J. Nanotechnol 2018, 9, 311–320. [PubMed: 29441274]

(33). Xu X; Yang Q; Cheung KM; Zhao C; Wattanatorn N; Belling JN; Abendroth JM; Slaughter LS; Mirkin CA; Andrews AM; Weiss PS Polymer-Pen Chemical Lift-Off Lithography. Nano Lett. 2017, 17, 3302–3311. [PubMed: 28409640]

(34). Zhao C; Xu X; Yang Q; Man T; Jonas SJ; Schwartz JJ; Andrews AM; Weiss PS Self-Collapse Lithography. Nano Lett. 2017, 17, 5035–5042. [PubMed: 28737930]

(35). Cao HH; Nakatsuka N; Serino AC; Liao W-S; Cheunkar S; Yang H; Weiss PS; Andrews AM Controlled DNA Patterning by Chemical Lift-Off Lithography: Matrix Matters. ACS Nano 2015, 9, 11439–11454. [PubMed: 26426585]

(36). Abendroth JM; Nakatsuka N; Ye M; Kim D; Fullerton EE; Andrews AM; Weiss PS Analyzing Spin Selectivity in DNA-Mediated Charge Transfer *via* Fluorescence Microscopy. ACS Nano 2017, 11, 7516–7526. [PubMed: 28672111]

(37). Chen C-Y; Wang C-M; Chen P-S; Liao W-S Surface Functional DNA Density Control by Programmable Molecular Defects. Chem. Commun 2018, 54, 4100–4103.

(38). Chen C-Y; Wang C-M; Chen P-S; Liao W-S Self-Standing Aptamers by an Artificial Defect-Rich Matrix. Nanoscale 2018, 10, 3191–3197. [PubMed: 29372203]

(39). Cao HH; Nakatsuka N; Deshayes S; Abendroth JM; Yang H; Weiss PS; Kasko AM; Andrews AM Small-Molecule Patterning via Prefunctionalized Alkanethiols. Chem. Mater 2018, 30, 4017–4030. [PubMed: 30828130]

(40). Kim J; Rim YS; Chen H; Cao HH; Nakatsuka N; Hinton HL; Zhao C; Andrews AM; Yang Y; Weiss PS Fabrication of High-Performance Ultrathin In_2O_3 Film Field-Effect Transistors and Biosensors Using Chemical Lift-Off Lithography. ACS Nano 2015, 9, 4572–4582. [PubMed: 25798751]

(41). Zhao C; Xu X; Bae S-H; Yang Q; Liu W; Belling JN; Cheung KM; Rim YS; Yang Y; Andrews AM; Weiss PS Large-Area, Ultrathin Metal-Oxide Semiconductor Nanoribbon Arrays Fabricated by Chemical Lift-Off Lithography. Nano Lett. 2018, 18, 5590–5595. [PubMed: 30060654]

(42). Kim E; Park K; Hwang S Electrochemical Investigation of Chemical Lift-off Lithography on Au and ITO. Electrochim. Acta 2017, 246, 165–172.

(43). Nguyen HM; Park K; Hwang S The Effect of an Antigalvanic Reduction of Silver on Gold for the Stability of a Self-Assembled Alkanethiol Monolayer and Chemical Lift-Off Lithography. J. Phys. Chem. C 2018, 122, 16070–16078.

(44). Laibinis PE; Fox MA; Folkers JP; Whitesides GM Comparisons of Self-Assembled Monolayers on Silver and Gold: Mixed Monolayers Derived from $HS(CH_2)_{21}X$ and $HS(CH_2)_{10}Y$ (X, Y = CH_3, CH_2OH) Have Similar Properties. Langmuir 1991, 7, 3167–3173.

(45). Laibinis PE; Whitesides GM; Allara DL; Tao YT; Parikh AN; Nuzzo RG Comparison of the Structures and Wetting Properties of Self-Assembled Monolayers of *n*-Alkanethiols on the Coinage Metal Surfaces, Copper, Silver, and Gold. J. Am. Chem. Soc 1991, 113, 7152–7167.

(46). Laibinis PE; Whitesides GM Self-Assembled Monolayers of *n*-Alkanethiolates on Copper Are Barrier Films That Protect the Metal against Oxidation by Air. J. Am. Chem. Soc 1992, 114, 9022–9028.

(47). Xia Y; Zhao X-M; Whitesides GM Pattern Transfer: Self-Assembled Monolayers as Ultrathin Resists. Microelectron. Eng 1996, 32, 255–268.

(48). Love JC; Wolfe DB; Chabinyc ML; Paul KE; Whitesides GM Self-Assembled Monolayers of Alkanethiolates on Palladium Are Good Etch Resists. J. Am. Chem. Soc 2002, 124, 1576–1577. [PubMed: 11853422]

(49). Love JC; Wolfe DB; Haasch R; Chabinyc ML; Paul KE; Whitesides GM; Nuzzo RG Formation and Structure of Self-Assembled Monolayers of Alkanethiolates on Palladium. J. Am. Chem. Soc 2003, 125, 2597–2609. [PubMed: 12603148]

(50). Schneeweiss MA; Rubinstein I In *Encyclopedia of Electrochemistry*; Bard AJ, Ed., 2007; DOI:10.1002/9783527610426.bard100109.

(51). Xia Y; Kim E; Whitesides GM Microcontact Printing of Alkanethiols on Silver and Its Application in Microfabrication. J. Electrochem. Soc. 1996, 143, 1070–1079.

(52). Xia Y; Kim E; Mrksich M; Whitesides GM Microcontact Printing of Alkanethiols on Copper and Its Application in Microfabrication. Chem. Mater. 1996, 8, 601–603.

(53). Mekhalif Z; Riga J; Pireaux JJ; Delhalle J Self-Assembled Monolayers of *n*-Dodecanethiol on Electrochemically Modified Polycrystalline Nickel Surfaces. Langmuir 1997, 13, 2285–2290.

(54). Mekhalif Z; Delhalle J; Lang P; Garnier F; Pireaux JJ Comparative Study of the Electrodeposition of Polybithiophene Films on Titanium Electrodes: Bare and Modified with Aromatic and Aliphatic Thiols. Synth. Met 1998, 96, 165–175.

(55). Mekhalif Z; Delhalle J; Lang P; Garnier F; Caudano R Electropolymerization of Bithiophene on Aluminum Surfaces Modified by $CH_3(CH_2)_9$—SH and ϕ—$(CH_2)_m$—SH, m = 0 to 3. J. Electrochem. Soc. 1999, 146, 2913–2918.

(56). Lee N; Choi S; Kang S Self-Assembled Monolayer as an Antiadhesion Layer on a Nickel Nanostamper in the Nanoreplication Process for Optoelectronic Applications. Appl. Phys. Lett 2006, 88, 073101.

(57). Rajalingam S; Devillers S; Dilimon VS; Delhalle J; Mekhalif Z Self-Assembled Monolayers of *n*-Dodecanethiol on Nickel Surfaces Using 2-Hydroxyethylammonium Formate as Reducing Medium. J. Electrochem. Soc 2017, 164, E36–E41.

(58). Abendroth JM; Cheung KM; Stemer DM; El Hadri MS; Zhao C; Fullerton EE; Weiss PS Spin-Dependent Ionization of Chiral Molecular Films. J. Am. Chem. Soc 2019, 141, 3863–3874. [PubMed: 30734553]

(59). Nakatsuka N; Yang K-A; Abendroth JM; Cheung KM; Xu X; Yang H; Zhao C; Zhu B; Rim YS; Yang Y; Weiss PS; Stojanović MN; Andrews AM Aptamer–Field-Effect Transistors Overcome Debye Length Limitations for Small-Molecule Sensing. Science 2018, 362, 319–324. [PubMed: 30190311]

(60). Cheung KM; Yang K-A; Nakatsuka N; Zhao C; Ye M; Jung ME; Yang H; Weiss PS; Stojanović MN; Andrews AM Phenylalanine Monitoring via Aptamer-Field-Effect Transistor Sensors. ACS Sensors 2019, DOI:10.1021/acssensors.9b01963.

(61). Han P; Akagi K; Federici Canova F; Shimizu R; Oguchi H; Shiraki S; Weiss PS; Asao N; Hitosugi T Self-Assembly Strategy for Fabricating Connected Graphene Nanoribbons. ACS Nano 2015, 9, 12035–12044. [PubMed: 26588477]

(62). Zhang H Ultrathin Two-Dimensional Nanomaterials. ACS Nano 2015, 9, 9451–9469. [PubMed: 26407037]

(63). Li Z; Chang S-C; Williams RS Self-Assembly of Alkanethiol Molecules onto Platinum and Platinum Oxide Surfaces. Langmuir 2003, 19, 6744–6749.

(64). Petrovykh DY; Kimura-Suda H; Opdahl A; Richter LJ; Tarlov MJ; Whitman LJ Alkanethiols on Platinum: Multicomponent Self-Assembled Monolayers. Langmuir 2006, 22, 2578–2587. [PubMed: 16519457]

(65). Gorman CB; Biebuyck HA; Whitesides GM Use of a Patterned Self-Assembled Monolayer To Control the Formation of a Liquid Resist Pattern on a Gold Surface. Chem. Mater. 1995, 7, 252–254.

(66). Köllensperger PA; Karl WJ; Ahmad MM; Pike WT; Green M Patterning of Platinum (Pt) Thin Films by Chemical Wet Etching in Aqua Regia. J. Micromech. Microeng 2012, 22, 067001.

(67). Shaheen A; Sturm JM; Ricciardi R; Huskens J; Lee CJ; Bijkerk F Characterization of Self-Assembled Monolayers on a Ruthenium Surface. Langmuir 2017, 33, 6419–6426. [PubMed: 28585831]

(68). Hohman JN; Kim M; Bednar HR; Lawrence JA; McClanahan PD; Weiss PS Simple, Robust Molecular Self-Assembly on Germanium. Chem. Sci 2011, 2, 1334–1343.

(69). Han SM; Ashurst WR; Carraro C; Maboudian R Formation of Alkanethiol Monolayer on Ge(111). J. Am. Chem. Soc 2001, 123, 2422–2425. [PubMed: 11456892]

(70). Ardalan P; Musgrave CB; Bent SF Formation of Alkanethiolate Self-Assembled Monolayers at Halide-Terminated Ge Surfaces. Langmuir 2009, 25, 2013–2025. [PubMed: 19152272]

(71). Nathan Hohman J; Kim M; Lawrence JA; McClanahan PD; Weiss PS High-Fidelity Chemical Patterning on Oxide-Free Germanium. J. Phys.: Condens. Matter 2012, 24, 164214. [PubMed: 22466616]

(72). Kim J; Rim YS; Liu Y; Serino AC; Thomas JC; Chen H; Yang Y; Weiss PS Interface Control in Organic Electronics Using Mixed Monolayers of Carboranethiol Isomers. Nano Lett. 2014, 14, 2946–2951. [PubMed: 24773449]

(73). Serino AC; Anderson ME; Saleh LMA; Dziedzic RM; Mills H; Heidenreich LK; Spokoyny AM; Weiss PS Work Function Control of Germanium through Carborane-Carboxylic Acid Surface Passivation. ACS Appl. Mater. Interfaces 2017, 9, 34592–34596. [PubMed: 28920673]

(74). Borchert AM; Vecchio KS; Stein RD The Use of Charging Effects in Al/Al2O3 Metal-Matrix Composites as a Contrast Mechanism in the SEM. Scanning 1991, 13, 344–349.

(75). Abe H; Babin S; Borisov S; Hamaguchi A; Kadowaki M; Miyano Y; Yamazaki Y Contrast Reversal Effect in Scanning Electron Microscopy Due to Charging. J. Vac. Sci. Technol., B 2009, 27, 1039–1042.

(76). Kim KH; Akase Z; Suzuki T; Shindo D Charging Effects on SEM/SIM Contrast of Metal/Insulator System in Various Metallic Coating Conditions. Mater. Trans 2010, 51, 1080–1083.

(77). Hovis JS; Boxer SG Patterning Barriers to Lateral Diffusion in Supported Lipid Bilayer Membranes by Blotting and Stamping. Langmuir 2000, 16, 894–897.

(78). Rogers JA Nanometer-Scale Printing. Science 2012, 337, 1459–1460. [PubMed: 22997312]

(79). Carlson A; Bowen AM; Huang Y; Nuzzo RG; Rogers JA Transfer Printing Techniques for Materials Assembly and Micro/Nanodevice Fabrication. Adv. Mater 2012, 24, 5284–5318. [PubMed: 22936418]

(80). Meitl MA; Zhu Z-T; Kumar V; Lee KJ; Feng X; Huang YY; Adesida I; Nuzzo RG; Rogers JA Transfer Printing by Kinetic Control of Adhesion to an Elastomeric Stamp. Nature Materials 2006, 5, 33–38.

(81). Stranick SJ; Parikh AN; Allara DL; Weiss PS A New Mechanism for Surface Diffusion: Motion of a Substrate-Adsorbate Complex. J. Phys. Chem 1994, 98, 11136–11142.

(82). Dean JA Lange's Handbook of Chemistry, 15th *ed.*; McGraw-Hill: New York, 1998.

(83). Skulason H; Frisbie CD Detection of Discrete Interactions upon Rupture of Au Microcontacts to Self-Assembled Monolayers Terminated with $-S(CO)CH_3$ or −SH. J. Am. Chem. Soc 2000, 122, 9750–9760.

(84). Bianco E; Butler S; Jiang S; Restrepo OD; Windl W; Goldberger JE Stability and Exfoliation of Germanane: A Germanium Graphane Analogue. ACS Nano 2013, 7, 4414–4421. [PubMed: 23506286]

(85). Dameron AA; Hampton JR; Gillmor SD; Hohman JN; Weiss PS Enhanced Molecular Patterning via Microdisplacement Printing. J. Vac. Sci. Technol., B 2005, 23, 2929–2932.

(86). Yang Q Ph.D. Dissertation, University of California, Los Angeles, Los Angeles, Califronia, 2018.

(87). Chen JG; Menning CA; Zellner MB Monolayer Bimetallic Surfaces: Experimental and Theoretical Studies of Trends in Electronic and Chemical Properties. Surf. Sci. Rep 2008, 63, 201–254.

(88). Kataby G; Prozorov T; Koltypin Y; Cohen H; Sukenik CN; Ulman A; Gedanken A Self-Assembled Monolayer Coatings on Amorphous Iron and Iron Oxide Nanoparticles: Thermal Stability and Chemical Reactivity Studies. Langmuir 1997, 13, 6151–6158.

(89). Nogues C; Lang P Self-Assembled Alkanethiol Monolayers on a Zn Substrate: Structure and Organization. Langmuir 2007, 23, 8385–8391. [PubMed: 17595122]

(90). Devillers S; Hennart A; Delhalle J; Mekhalif Z 1-Dodecanethiol Self-Assembled Monolayers on Cobalt. Langmuir 2011, 27, 14849–14860. [PubMed: 22040160]

(91). Baum T; Ye S; Uosaki K Formation of Self-Assembled Monolayers of Alkanethiols on GaAs Surface with in Situ Surface Activation by Ammonium Hydroxide. Langmuir 1999, 15, 8577–8579.

(92). Presolski S; Pumera M Covalent Functionalization of MoS2. Mater. Today 2016, 19, 140–145.

(93). Thomas JC; Goronzy DP; Dragomiretskiy K; Zosso D; Gilles J; Osher SJ; Bertozzi AL; Weiss PS Mapping Buried Hydrogen-Bonding Networks. ACS Nano 2016, 10, 5446–5451. [PubMed: 27096290]

(94). Thomas JC; Schwartz JJ; Hohman JN; Claridge SA; Auluck HS; Serino AC; Spokoyny AM; Tran G; Kelly KF; Mirkin CA; Gilles J; Osher SJ; Weiss PS Defect-Tolerant Aligned Dipoles within Two-Dimensional Plastic Lattices. ACS Nano 2015, 9, 4734–4742. [PubMed: 25867638]

(95). Thomas JC; Boldog I; Auluck HS; Bereciartua PJ; Dušek M; Macháček J; Bastl Z; Weiss PS; Baše T Self-Assembled *p*-Carborane Analogue of *p*-Mercaptobenzoic Acid on Au{111}. Chem. Mater 2015, 27, 5425–5435.

(96). Thomas JC; Goronzy DP; Serino AC; Auluck HS; Irving OR; Jimenez-Izal E; Deirmenjian JM; Macháček J; Sautet P; Alexandrova AN; Baše T; Weiss PS Acid–Base Control of Valency within Carboranedithiol Self-Assembled Monolayers: Molecules Do the Can-Can. ACS Nano 2018, 12, 2211–2221. [PubMed: 29393628]

(97). Gao W; Dickinson L; Grozinger C; Morin FG; Reven L Self-Assembled Monolayers of Alkylphosphonic Acids on Metal Oxides. Langmuir 1996, 12, 6429–6435.

(98). Mandziak A; de la Figuera J; Ruiz-Gómez S; Soria GD; Pérez L; Prieto P; Quesada A; Foerster M; Aballe L Structure and Magnetism of Ultrathin Nickel-Iron Oxides Grown on Ru(0001) by High-Temperature Oxygen-Assisted Molecular Beam Epitaxy. Sci. Rep 2018, 8, 17980. [PubMed: 30568169]

(99). Chen C-Y; Chang C-H; Wang C-M; Li Y-J; Chu H-Y; Chan H-H; Huang Y-W; Liao W-S Large Area Nanoparticle Alignment by Chemical Lift-Off Lithography. Nanomaterials 2018, 8, 71.

(100). Ashley MJ; Bourgeois MR; Murthy RR; Laramy CR; Ross MB; Naik RR; Schatz GC; Mirkin CA Shape and Size Control of Substrate-Grown Gold Nanoparticles for Surface-Enhanced Raman Spectroscopy Detection of Chemical Analytes. J. Phys. Chem. C 2018, 122, 2307–2314.

(101). Ohnsorg ML; Beaudoin CK; Anderson ME Fundamentals of MOF Thin Film Growth *via* Liquid-Phase Epitaxy: Investigating the Initiation of Deposition and the Influence of Temperature. Langmuir 2015, 31, 6114–6121. [PubMed: 26020573]

(102). Hatzor A; Weiss PS Molecular Rulers for Scaling Down Nanostructures. Science 2001, 291, 1019–1020. [PubMed: 11161210]

(103). Lau J; Trojniak AE; Maraugha MJ; VanZanten AJ; Osterbaan AJ; Serino AC; Ohnsorg ML; Cheung KM; Ashby DS; Weiss PS; Dunn BS; Anderson ME Conformal Ultrathin Film MOF Analogs: Characterization of Growth, Porosity, and Electronic Transport. Chem. Mater 2019, DOI:10.1021/acs.chemmater.9b03141 10.1021/acs.chemmater.9b03141.

(104). Trang B; Yeung M; Popple DC; Schriber EA; Brady MA; Kuykendall TR; Hohman JN Tarnishing Silver Metal into Mithrene. J. Am. Chem. Soc 2018, 140, 13892–13903. [PubMed: 30265001]

(105). Nečas D; Klapetek P Gwyddion: An Open-Source Software for SPM Data Analysis. Cent. Eur. J. Phys 2012, 10, 181–188.

(106). Goldstein JI; Newbury DE; Michael JR; Ritchie NWM; Scott JHJ; Joy DC In *Scanning Electron Microscopy and X-Ray Microanalysis*; Goldstein JI; Newbury DE; Michael JR; Ritchie NWM; Scott JHJ; Joy DC, Eds.; Springer New York: New York, NY, 2018; pp 123–131.

(107). Shankoff T Chemical Etchant for Palladium. US3839110A, 10 1, 1974.

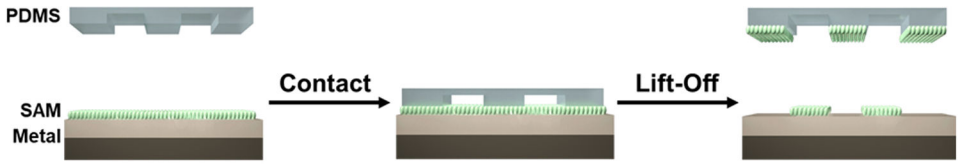

Figure 1.

General scheme for chemical lift-off lithography. An oxygen-plasma-activated polydimethylsiloxane (PDMS) stamp is brought into contact with a metal or semiconductor surface functionalized with a self-assembled monolayer (SAM), in this case, 11-mercapto-1-undecanol. Lift-off of the PDMS stamp removes SAM molecules only in the contacted regions, patterning remaining SAMs on the substrate surfaces.

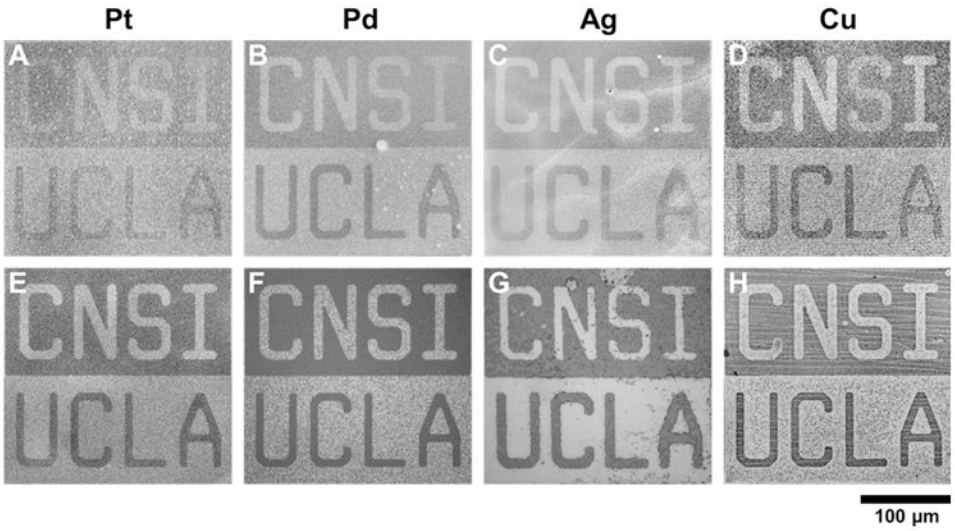

Figure 2.

Chemical lift-off lithography (CLL) of coinage metal (Pt, Pd, Ag, Cu) surfaces. Metals are ordered in terms of increasing reactivity from left to right. **(A-D)** Representative scanning electron microscopy images of patterned self-assembled monolayers (SAMs) of 11-mercapto-1-undecanol (MUO) on metal surfaces after CLL. Monolayers were patterned such that MUO molecules remained in the "CNSI" letter regions and in the regions surrounding the "UCLA" letters. **(E-H)** Representative optical microscopy images of metal surfaces after chemical wet etching using the patterned SAMs as molecular resists.

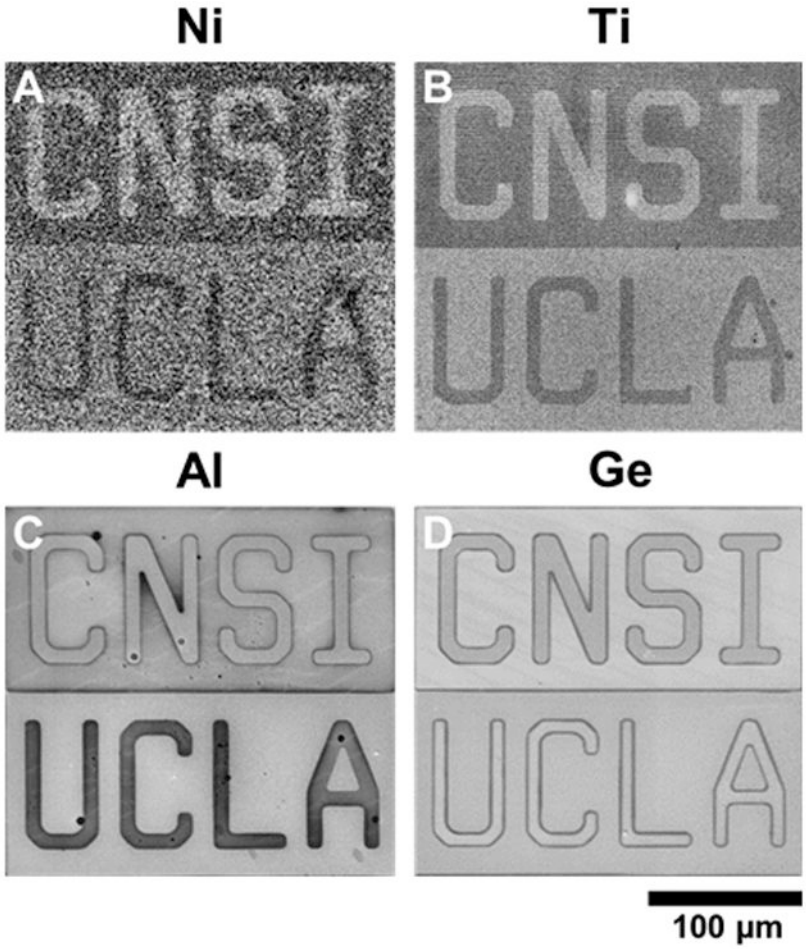

Figure 3.

Chemical lift-off lithography (CLL) of transition or reactive metal and semiconductor surfaces. **(A-D)** Representative scanning electron microscopy images of patterned self-assembled monolayers of 11-mercapto-1-undecanol on the metal surfaces (Ni, Ti, Al) and a semiconductor surface (Ge) after CLL. Stamps with the same features as Figure 2 were used.

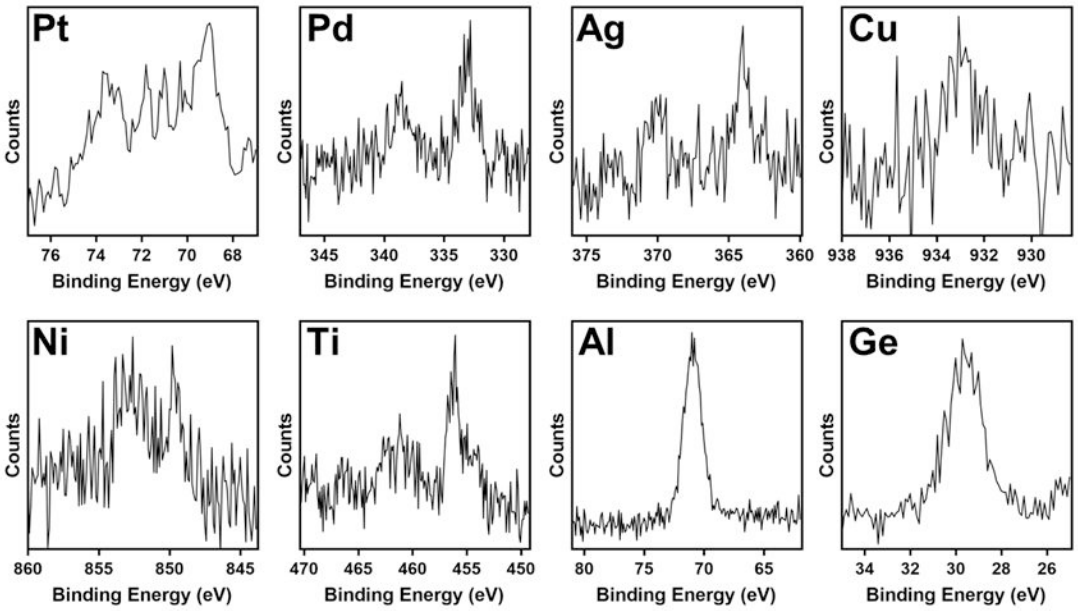

Figure 4.

X-ray photoelectron spectroscopy (XPS) analysis of featureless polydimethylsiloxane (PDMS) stamps after a chemical lift-off lithography on Pt, Pd, Ag, Cu, Ni, Ti, Al, and Ge surfaces. Featureless PDMS stamps and XPS were used to investigate the presence of corresponding substrate atoms on the PDMS stamps, demonstrating that layers of substrate atoms are removed in the lift-off process, either nominal monolayers, or in some cases, potentially thicker layers.

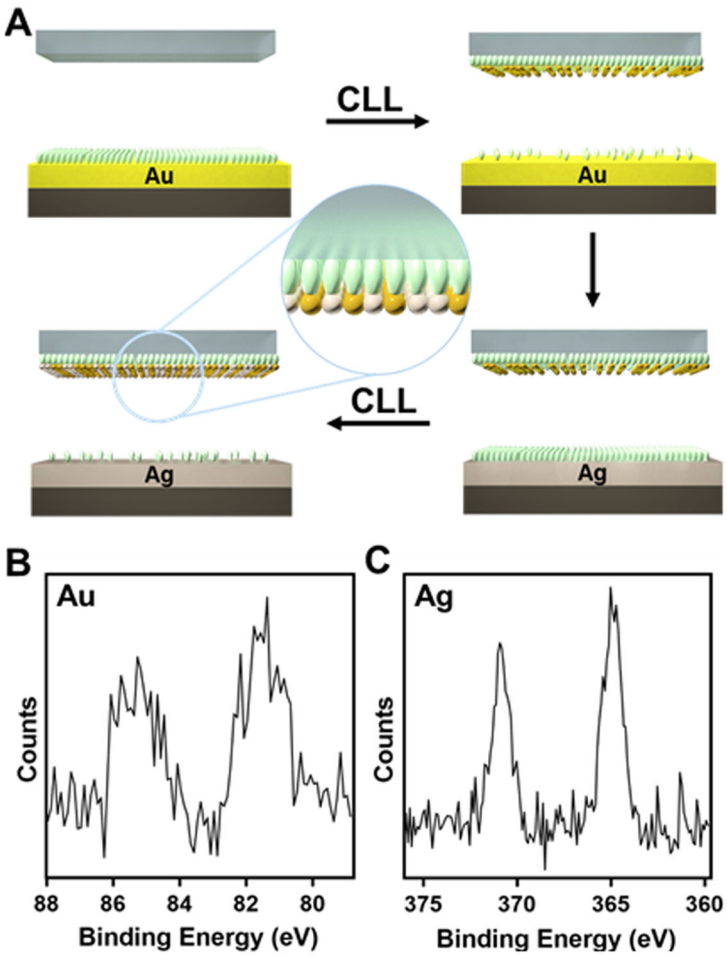

Figure 5.

Sequential chemical lift-off lithography (CLL) of two different metals (Au, Ag) onto the same polydimethylsiloxane (PDMS) stamp. **(A)** Schematic illustration of the sequential CLL process. **(B,C)** X-ray photoelectron spectra of the PDMS stamp after the sequential CLL process showing characteristic peaks of both metals on the same stamp, demonstrating that both metals are “lifted-off” onto the PDMS stamp forming a supported mixed metal monolayer.